PATTERN RECOGNITION OF RANDOM SPATIAL SIGNALS USING COHERENT OPTICAL TECHNIQUES

In Progress Report 1 (PR1) it was shown how biological photomicrographs could be considered to be random diffracting screens when illuminated with coherent light. This is a particular example of the general problem of pattern recognition of random spatial signals. The main purpose of current research is to determine to what extent statistical analysis and identification of random spatial signals can be carried out by optical techniques. The development of such techniques would be important for a wide variety of possible applications. As described in PR1 application of these techniques to biological photomicrographs would permit the direct determination of such statistical quantities as mean cell size and distribution.

Another area of application of these techniques is to provide a quantitative measure of "randomness" to be used as an error signal in automatic control systems. For example, the total light scattered off-axis in the transform plane provides a direct measure of the variance of the random process. Such measurements could provide an index of smoothness of reflecting surfaces. Based on such an index, for example, a spacecraft might be landed automatically on the smoothest terrain of a moon or planet. Another spatially random control signal might

be the distribution of stars in the sky. If different regions of the sky have different statistical distributions of stars, then direct optical measurements of these properties might be used in the automatic control and navigation of spacecraft.

In PR1 it was shown how an optical processing system could be used for power spectrum and autocorrelation measurements. The standard optical processing system contains a collimating lens, a transforming lens, and an imaging (or second transforming) lens. By appropriately locating the input plane, the same lens can be used for both transforming and imaging the input signal. As will be shown below, the incident wave need not be a plane wave so that the collimating lens can also be eliminated. An analysis of this system will allow one to determine the relationship between the spatial frequency in the power spectrum measurements and the geometry of the system.

A schematic of the optical processing system is shown in Figure 1 where $\underset{\sim}{g}(x,y)$ is the complex transmittance of the photomicrograph or other random spatial signal. The single lens in this system could be replaced by a spherical mirror resulting in the lensless optical processor discussed in PR1. Such a system could be designed to accept photomicrographs of large spatial extent thus justifying the ergodic hypothesis when making power spectrum measurements of random signals. The analysis below applies to either a single lens system or a lensless system using a spherical mirror.

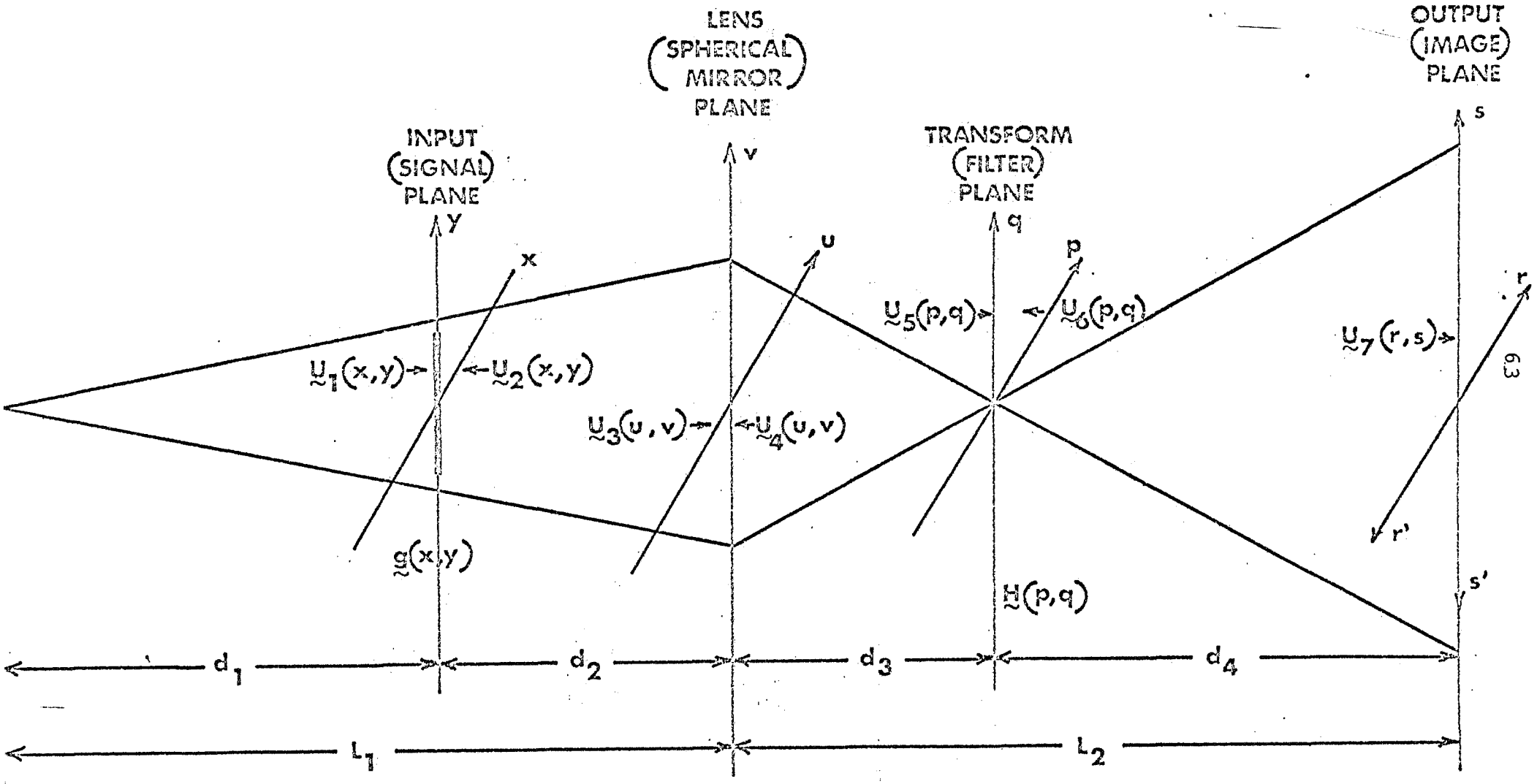

Fig. 1 Geometry of Single Lens Optical Processor

Analysis of the Optical Processing System

A wave analysis of the optical system in Figure 1 can be carried out by determining the complex amplitude of the wave $\underset{\sim}{U}(x,y)$ at any plane perpendicular to the optical axis. If $\underset{\sim}{U}'(x_1,y_1)$ is the complex amplitude of the wave at plane z = 0, then the complex amplitude $\underset{\sim}{U}(x_o,y_o)$ at a parallel plane a distance z away is given by the Huygen-Fresnel principle[1,2] as shown in Figure 2. Referring to Figure 2 one sees that the effect of traveling a distance d in free space is to change $\underset{\sim}{U}'(x_1,y_1)$ to $\underset{\sim}{U}(x_o,y_o)$ through the relation

$$\underset{\sim}{U}(x_o,y_o) = \underset{\sim}{K} \iint_{-\infty}^{\infty} \underset{\sim}{U}'(x_1,y_1) e^{j\frac{k}{2d}[(x_o-x_1)^2 + (y_o-y_1)^2]} dx_1 dy_1 \qquad (1)$$

where $\underset{\sim}{K}$ is a complex constant and $\underset{\sim}{U}'(x_1,y_1)$ is assumed to be zero outside the aperture. The result for light from a point source on the axis traveling a distance d is found by letting $\underset{\sim}{U}'(x_1,y_1) = \delta(x_1,y_1)$ in (1) from which

$$\underset{\sim}{U}_d(x_o,y_o) = \underset{\sim}{K}\, e^{j\frac{k}{2d}(x_o^2 + y_o^2)} \qquad (2)$$

The effect of the lens (or spherical mirror) is to multiply the incident amplitude function $\underset{\sim}{U}(x,y)$ by some complex amplitude $\underset{\sim}{\psi}(x,y)$. To determine $\underset{\sim}{\psi}(x,y)$ recognize that light from a point source which is incident on the lens (or mirror) after traveling a distance f equal to the focal length will be transmitted (or reflected) as a plane wave. That is

Fig. 2 Geometry of Huygen-Fresnel principle

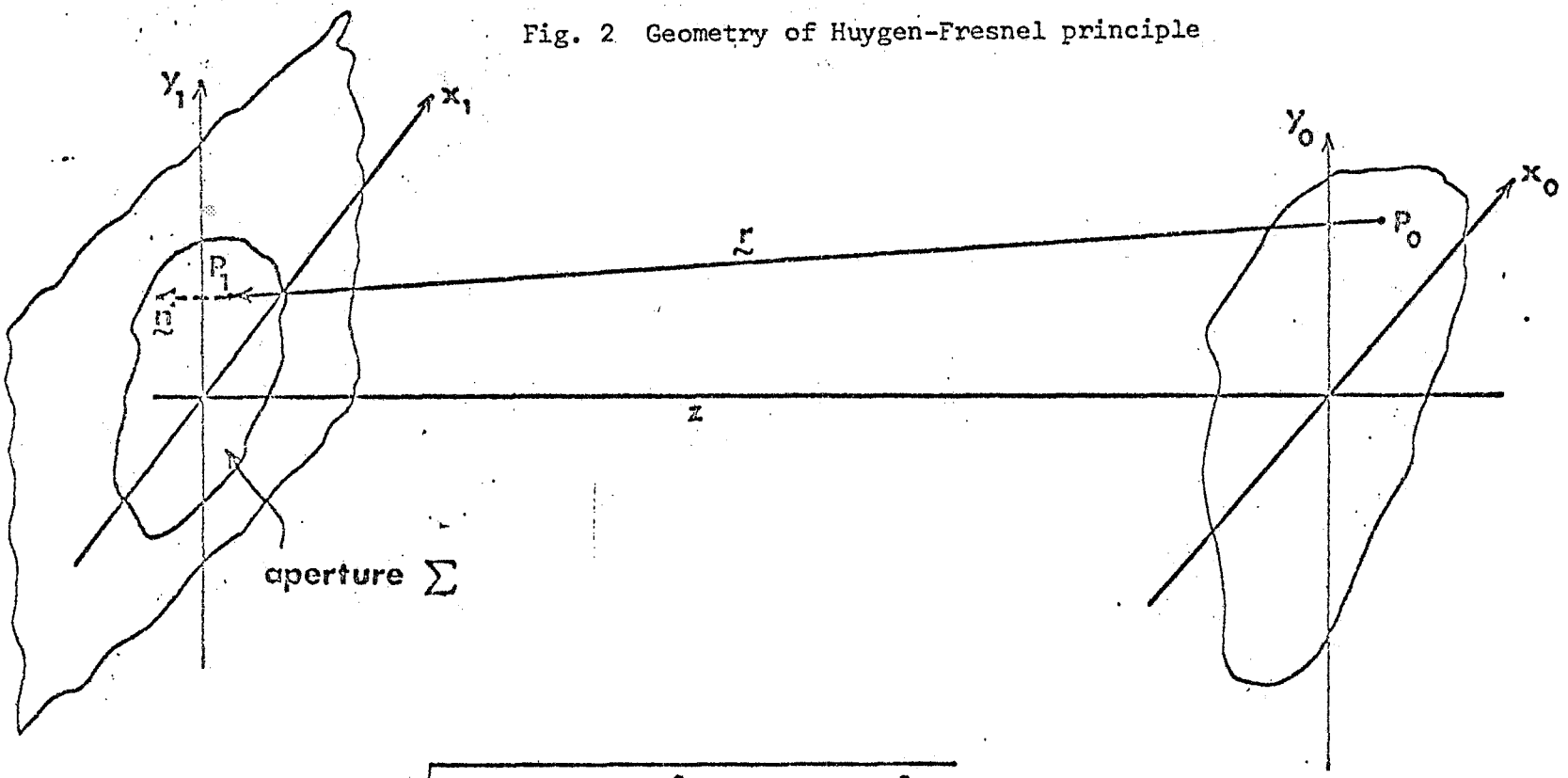

$$r = \sqrt{z^2 + (x_0 - x_1)^2 + (y_0 - y_1)^2}$$

$$\approx z\left[1 + \frac{1}{2}\left(\frac{x_0 - x_1}{z}\right)^2 + \frac{1}{2}\left(\frac{y_0 - y_1}{z}\right)^2\right] \qquad \text{(Paraxial Approximation)}$$

$$\underset{\sim}{U}(x_0, y_0) = \frac{1}{j\lambda}\iint_{\Sigma} \underset{\sim}{U}'(x_1, y_1)\,\frac{e^{jkr}}{r}\cos(\underset{\sim}{n}, \underset{\sim}{r})\,dx_1\,dy_1$$

$$\approx \frac{e^{jkz}}{j\lambda z}\iint_{-\infty}^{\infty} \underset{\sim}{U}'(x_1, y_1)\; e^{j\frac{k}{2z}\left[(x_0 - x_1)^2 + (y_0 - y_1)^2\right]}\,dx_1\,dy_1$$

$$\underset{\sim}{U}_f(x,y)\ \underset{\sim}{\psi}(x,y) = \text{constant}$$

and thus from (2) it follows that

$$\underset{\sim}{\psi}(x,y) = e^{-j\frac{k}{2f}(x^2 + y^2)} \tag{3}$$

represents the effect of the lens (or spherical mirror) where f is the focal length of the lens (or mirror).

Refer now to Figure 1 where $\underset{\sim}{U}_1(x,y)$ is the light amplitude just to the left of the signal plane. From (2) $\underset{\sim}{U}_1(x,y)$ is given by

$$\underset{\sim}{U}_1(x,y) = \underset{\sim}{K}_1\, e^{j\frac{k}{2d_1}(x^2 + y^2)} \tag{4}$$

To the right of the input plane $\underset{\sim}{U}_2(x,y)$ is given by

$$\underset{\sim}{U}_2(x,y) = \underset{\sim}{U}_1(x,y)\ \underset{\sim}{g}(x,y) \tag{5}$$

Equation (1) can be used to find $\underset{\sim}{U}_3(u,v)$ in terms of $\underset{\sim}{U}_2(x,y)$. Thus

$$\underset{\sim}{U}_3(u,v) = \underset{\sim}{K}_2 \iint_{-\infty}^{\infty} \underset{\sim}{U}_2(x,y)\, e^{j\frac{k}{2d_2}[(u-x)^2 + (v-y)^2]}\, dxdy \tag{6}$$

The effect of the lens (or mirror) is to multiply $\underset{\sim}{U}_3(u,v)$ by $\psi(u,v)$ given by (3). Thus

$$\underset{\sim}{U}_4(u,v) = \underset{\sim}{U}_3(u,v)\ e^{-j\frac{k}{2f}(u^2 + v^2)} \tag{7}$$

Using (1) again $\underset{\sim}{U}_5(p,q)$ can be written as

$$\underset{\sim}{U}_5(p,q) = \underset{\sim}{K}_3 \iint_{-\infty}^{\infty} \underset{\sim}{U}_4(u,v)\ e^{j\frac{k}{2d_3}[(p-u)^2 + (q-v)^2]}\ dudv \tag{8}$$

If a filter with a complex transmittance $\underset{\sim}{H}(p,q)$ is inserted in the p-q plane, then $\underset{\sim}{U}_6(p,q)$ is given by

$$\underset{\sim}{U}_6(p,q) = \underset{\sim}{U}_5(p,q)\ \underset{\sim}{H}(p,q) \tag{9}$$

Finally the light amplitude in the output plane $\underset{\sim}{U}_7(r,s)$ is given by

$$\underset{\sim}{U}_7(r,s) = \underset{\sim}{K}_4 \iint_{-\infty}^{\infty} \underset{\sim}{U}_6(p,q)\ e^{j\frac{k}{2d_4}[(r-p)^2 + (s-q)^2]} \tag{10}$$

It is convenient to first evaluate $\underset{\sim}{U}_5(p,q)$. Combining Equations (4) through (8) one can write

$$\underset{\sim}{U}_5(p,q) = \underset{\sim}{K}_5 \iiiint_{-\infty}^{\infty} \underset{\sim}{g}(x,y)\ e^{j\frac{k}{2}\rho}\ dudv\ dxdy \tag{11}$$

where

$$\rho = \frac{x^2 + y^2}{d_1} + \frac{u^2 + v^2 + x^2 + y^2 - 2ux - 2vy}{d_2} - \frac{u^2 + v^2}{f}$$

$$+ \frac{p^2 + q^2 + u^2 + v^2 - 2pu - 2qv}{d_3} \tag{12}$$

It is first necessary to do the integration over u and v. To this end let the parts of ρ containing u and v be represented by ρ_u and ρ_v respectively. Thus

$$\rho_u = u^2\left(\frac{1}{d_2} - \frac{1}{f} + \frac{1}{d_3}\right) - 2u\left(\frac{x}{d_2} + \frac{p}{d_3}\right)$$

$$\rho_v = v^2\left(\frac{1}{d_2} - \frac{1}{f} + \frac{1}{d_3}\right) - 2v\left(\frac{y}{d_2} + \frac{q}{d_3}\right) \qquad (13)$$

Since

$$\int_{-\infty}^{\infty} e^{jC_1(u-C_2)^2}\,du = C_3\int_{-\infty}^{\infty} e^{j\frac{\pi}{2}\xi^2}\,d\xi = \text{constant}$$

it is desirable to complete the squares in (13) and write

$$\rho_u = \rho_u' - \frac{d_2L_1}{d_1}\left(\frac{x}{d_2} + \frac{p}{d_3}\right)^2$$

$$\rho_v = \rho_v' - \frac{d_2L_1}{d_1}\left(\frac{y}{d_2} + \frac{q}{d_3}\right)^2 \qquad (14)$$

where

$$\rho_u' = \frac{d_1}{d_2L_1}\left[u - \frac{d_2L_1}{d_1}\left(\frac{x}{d_2} + \frac{p}{d_3}\right)\right]^2$$

$$\rho_v' = \frac{d_1}{d_2L_1}\left[u - \frac{d_2L_1}{d_1}\left(\frac{y}{d_2} + \frac{q}{d_3}\right)\right]^2 \qquad (15)$$

and the lens formula $1/f = 1/L_1 + 1/d_3$ has been used. Combining (14) with the remaining terms in (12) one can write ρ in the form

$$\rho = \rho_u' + \rho_v' + \left(\frac{1}{d_1} + \frac{1}{d_2} - \frac{L_1}{d_1d_2}\right)\left(x^2 + y^2\right)$$

$$+ \left(\frac{1}{d_3} - \frac{d_2L_1}{d_1d_3^2}\right)\left(p^2 + q^2\right) - \frac{2L_1}{d_1d_3}(xp + yq) \qquad (16)$$

The terms ρ_u' and ρ_v' give a constant when integrated over u and v. The coefficient of $(x^2 + y^2)$ in (16) is identically zero. Thus (11) can be written as

$$\underset{\sim}{U}_5(p,q) = \underset{\sim}{K}_6 \, e^{j\frac{k}{2d_3}\left(1 - \frac{d_2L_1}{d_1d_3}\right)\left(p^2 + q^2\right)} \iint_{-\infty}^{\infty} \underset{\sim}{g}(x,y) \, e^{-j\frac{2\pi L_1}{\lambda d_1 d_3}(xp + yq)} \, dxdy$$

$$= \underset{\sim}{K}_6 \, e^{j\frac{k}{2d_3}\left(1 - \frac{d_2L_1}{d_1d_3}\right)\left(p^2 + q^2\right)} \underset{\sim}{G}\left(\frac{L_1p}{\lambda d_1 d_3}, \frac{L_1q}{\lambda d_1 d_3}\right) \qquad (17)$$

where $\underset{\sim}{G}(f_x,f_y)$ is the two-dimensional Fourier transform of $\underset{\sim}{g}(x,y)$ with spatial frequencies $f_x = L_1p/\lambda d_1 d_3$ and $f_y = L_1q/\lambda d_1 d_3$.

A filter with an impulse response $\underset{\sim}{h}(x,y)$ and a transfer function $\underset{\sim}{H}(f_x,f_y)$ is to be inserted in the p-q plane. Then from (17), (9) and (10), $\underset{\sim}{U}_7(r,s)$ can be written as

$$\underset{\sim}{U}_7(r,s) = \underset{\sim}{K}_7 \iint_{-\infty}^{\infty} \underset{\sim}{G}\left(\frac{L_1p}{\lambda d_1 d_3}, \frac{L_1q}{\lambda d_1 d_3}\right) \underset{\sim}{H}\left(\frac{L_1p}{\lambda d_1 d_3}, \frac{L_1q}{\lambda d_1 d_3}\right) e^{j\frac{k}{2}u} \, dpdq \qquad (18)$$

where

$$u = \frac{1}{d_3}\left(1 - \frac{d_2L_1}{d_1d_3}\right)\left(p^2 + q^2\right) + \frac{1}{d_4}\left(r^2 + s^2 + p^2 + q^2 - 2rp - 2sq\right) \qquad (19)$$

The coefficient of $(p^2 + q^2)$ in (19) is

$$\frac{1}{d_3} + \frac{1}{d_4} - \frac{d_2 L_1}{d_1 d_3^2} \tag{20}$$

Applying the lens formula to Figure 1 one can write

$$\frac{1}{f} = \frac{1}{L_1} + \frac{1}{d_3} = \frac{1}{d_2} + \frac{1}{L_2} \tag{21}$$

By cross-multiplying and combining terms in (21) one can show that

$$\frac{L_1}{d_1 d_3} = \frac{L_2}{d_2 d_4} \tag{22}$$

Substituting (22) into (20) one obtains

$$\frac{1}{d_3} + \frac{1}{d_4} - \frac{L_2}{d_3 d_4} = 0$$

so that the coefficient of $(p^2 + q^2)$ in (19) vanishes. Thus, (18) reduces to

$$\underset{\sim}{U}_7(r,s) = \underset{\sim}{K}_7 \, e^{j\frac{k}{2d_4}(r^2 + s^2)} \iint_{-\infty}^{\infty} \underset{\sim}{G}\left(\frac{L_1 p}{\lambda d_1 d_3}, \frac{L_1 q}{\lambda d_1 d_3}\right) \underset{\sim}{H}\left(\frac{L_1 p}{\lambda d_1 d_3}, \frac{L_1 q}{\lambda d_1 d_3}\right)$$

$$e^{-j\frac{2\pi}{\lambda d_4}(rp + sq)} \, dpdq \tag{23}$$

In terms of the spatial frequencies $f_x = L_1 p/\lambda d_1 d_3$, $f_y = L_1 q/\lambda d_1 d_3$ and the reduced coordinates $r' = -(d_2/L_2)\, r$, $s' = -(d_2/L_2)\, s$ Equation (23) can be written as

$$\underset{\sim}{U}_7(r', s') = \underset{\sim}{K}_8 \, e^{j\frac{kL_2^2}{2d_4d_2^2}(r'^2 + s'^2)} \iint_{-\infty}^{\infty} \underset{\sim}{G}(f_x, f_y) \, \underset{\sim}{H}(f_x, f_y)$$

$$e^{j2\pi(f_x r' + f_y s')} \, df_x df_y \tag{24}$$

where (22) has been used. Thus to within a quadratic phase factor $\underset{\sim}{U}_7(r', s')$ is proportional to the inverse Fourier transform of the product $\underset{\sim}{G}(f_x, f_y) \, \underset{\sim}{H}(f_x, f_y)$. The light intensity in the output plane will therefore be proportional to the magnitude squared of this inverse Fourier transform or alternatively to the magnitude squared of the convolution of the input signal $\underset{\sim}{g}(x,y)$ with the impulse response $\underset{\sim}{h}(x,y)$. In particular, if no filter is used $\underset{\sim}{H}(p,q) = 1$, $\underset{\sim}{h}(x,y) = \delta(x,y)$ and the output intensity reduces to

$$I(r,s) = \left| \underset{\sim}{K}_8 \, \underset{\sim}{g}\left(-\frac{d_2}{L_2} r, \; - \frac{d_2}{L_2} s \right) \right|^2 \tag{25}$$

which as expected is an inverted image of $\underset{\sim}{g}(x,y)$ that has been magnified by an amount L_2/d_2.

Design Criteria for the Optical Processor

In designing the lensless processor for a particular application a compromise is often required between the magnification $M = L_2/d_2$, the actual size of the diffraction pattern in the transform (filter) plane, and the maximum spatial frequency that can be faithfully transmitted by the system in the

absence of any filtering in the transform plane. This maximum spatial frequency can be determined from the coherent transfer function which is equal to the pupil function of the spherical mirror $P(\lambda L_2 f_x', \lambda L_2 f_y')$[1,2]. This coherent transfer function is defined as the ratio of the frequency spectrum of the image to the frequency spectrum of the image predicted by geometrical optics. The spatial frequencies f_x' and f_y' are associated with the image coordinates. However, the spatial frequencies f_x and f_y related to the Fourier transform in (17) are associated with the input signal. These two sets of spatial frequencies are related by the magnification through the expression $f_{x,y} = Mf'_{x,y}$. Thus, in terms of the input spatial frequencies the coherent transfer function is given by $P(\lambda L_2 f_x/M, \lambda L_2 f_y/M) = P(\lambda d_2 f_x, \lambda d_2 f_y)$. For a lens (or spherical mirror) of diameter D the cut-off frequency f_o is thus given by

$$f_o = \frac{D}{2\lambda d_2} \tag{26}$$

This cut-off frequency f_o corresponds to the spatial frequency of an on-axis object whose diffracted light just makes it through the aperture of the lens (or spherical mirror). This is illustrated in Figure 3 where the solid line passing through the center of an object of width a belongs to the bundle of rays which converge to a point in the transfer plane at a distance p_o from the axis. This distance corresponds to the maximum spatial frequency

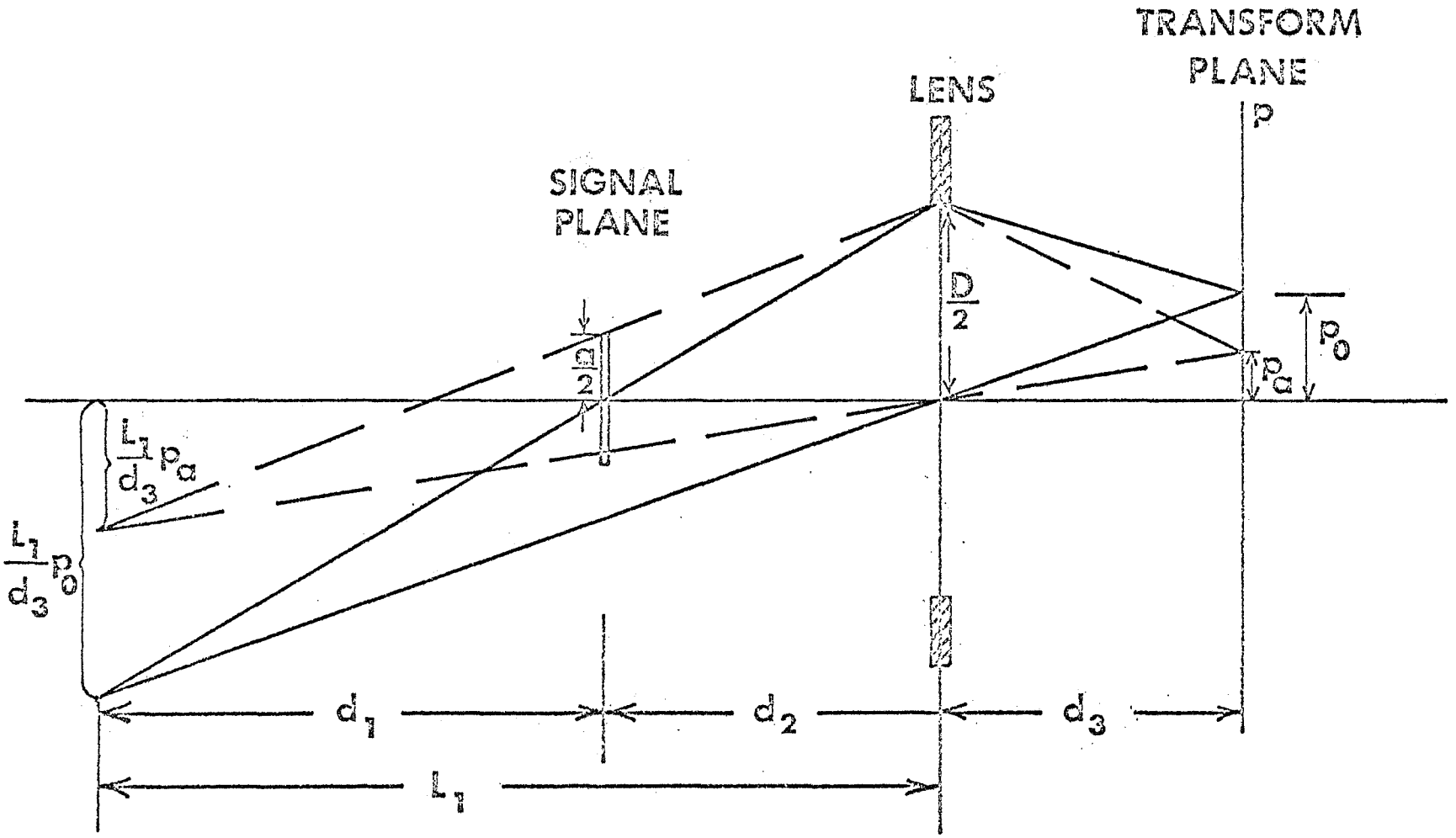

Fig. 3 Effect of lens aperture on maximum spatial frequency

$$f_o = \frac{L_1 p_o}{\lambda d_1 d_3} \tag{27}$$

which will be passed by an aperture of diameter D. From the geometry of Figure 3 one can readily show that

$$p_o = \frac{D\, d_1 d_3}{2\, d_2 L_1} \tag{28}$$

so that one can obtain (26) by substituting (28) into (27). Equation (26) is derived by considering the optical system to be space-invariant (isoplanatic). One would then expect this cut-off frequency f_o to apply to all points in the image. In fact, it does not as shown by the bundle of dashed rays in Figure 3. Light that is diffracted in the signal plane at a distance a/2 from the axis will only pass through the aperture of diameter D if the spatial frequency is less than $f_a = L_1 p_a / \lambda d_1 d_3$ as shown in Figure 3. From the geometry of this figure one can show that f_a is related to the cut-off frequency f_o given by (26) by the equation

$$f_a = f_o \left(1 - \frac{L_1}{d_1} \frac{a}{D}\right) \tag{29}$$

Thus the effect of the finite aperture is to reduce the maximum spatial frequency that can be faithfully transmitted by the system proportionately to the ratio a/D.

Optical Processing of Random Spatial Signals

A general computer technique has been developed for generating random spatial patterns with known statistical characteristics. The technique consists of locating a random point in a two dimensional space by means of an appropriate random function generator on a digital computer. Using a digital to analog converter voltages are obtained which automatically locate the random point as a spot on an oscilloscope face. A large number of random points can therefore be plotted rapidly and photographed by standard techniques. These techniques can be used, for example, to simulate the distribution of stars in different regions of the sky. Optical identification techniques can then be used to recognize the different random patterns.

One such pattern produced in this manner is shown in Figure 4. This pattern actually consists of a large number of two-spot patterns. The distance between the two spots in each case is a constant d. The orientation line joining the two spots is a random variable that is uniformly distributed from 0 to 2π radians. Thus this random pattern is a collection of the two-hole patterns described in PR 1.

The optical processing system described above was used to measure the power spectrum of this random dot pattern. The result as measured in the transform plane of Figure 2 is shown in Figure 5. The envelope of this power spectrum varies as

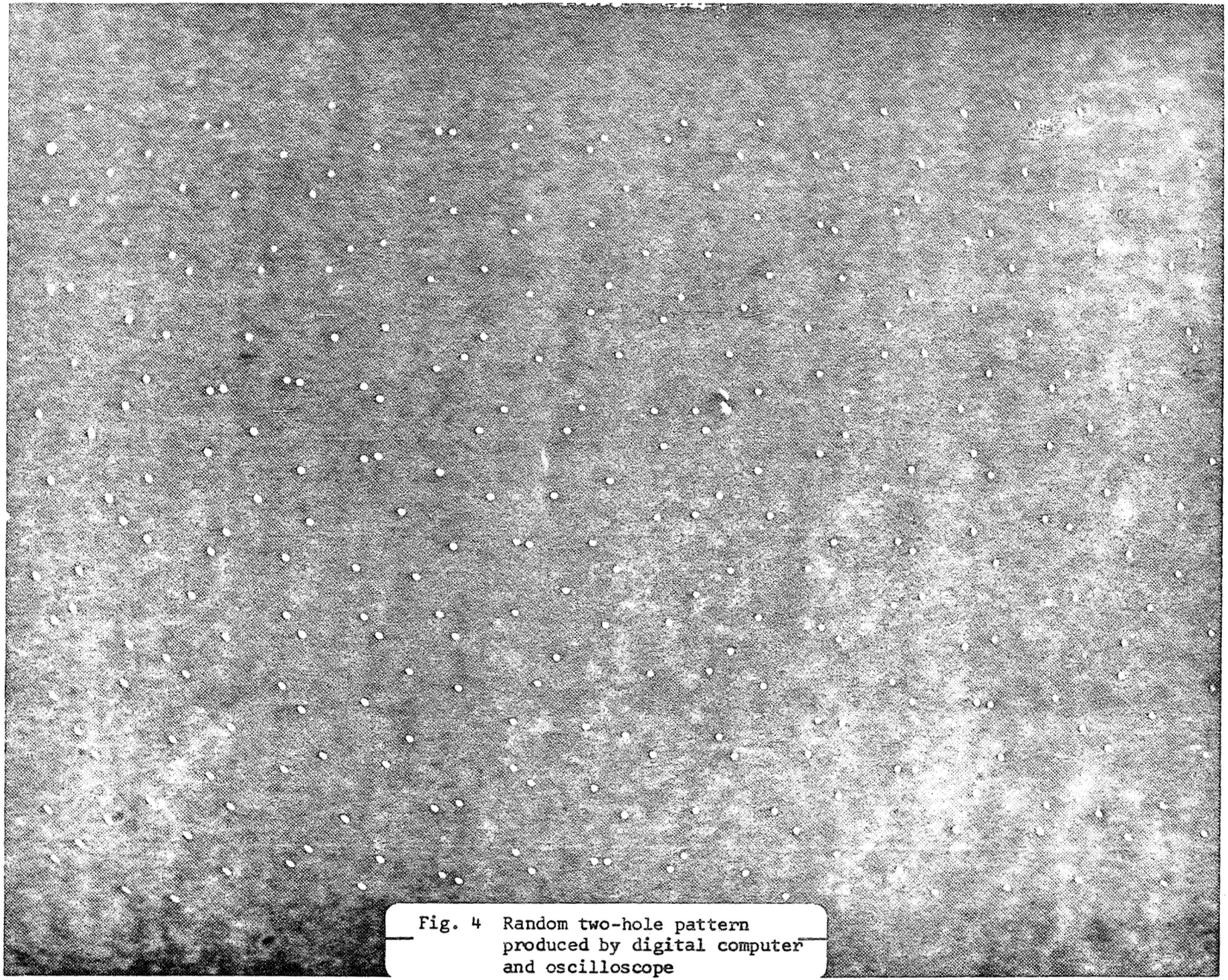

Fig. 4 Random two-hole pattern produced by digital computer and oscilloscope

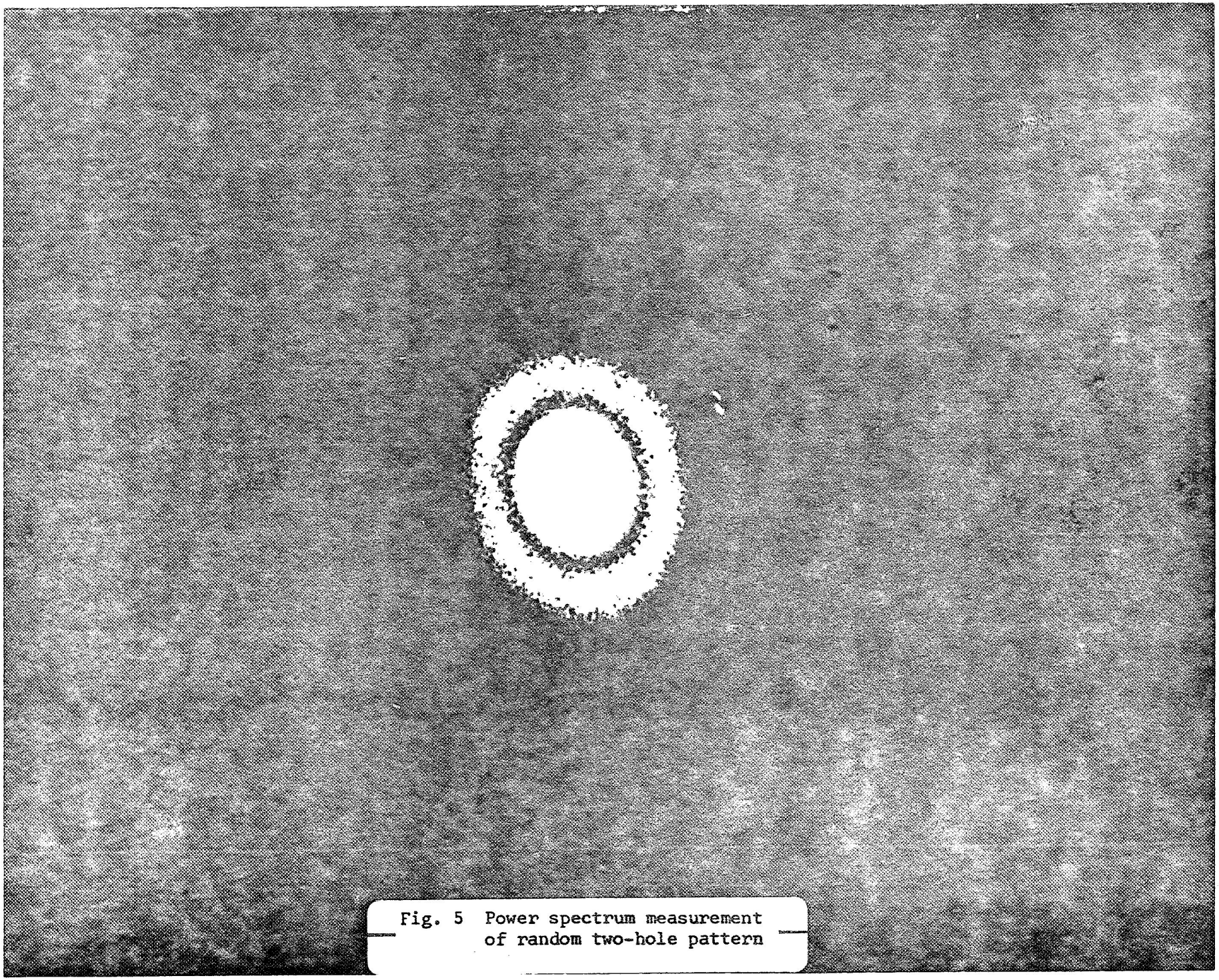

Fig. 5 Power spectrum measurement of random two-hole pattern

$[J_1(\pi af_o)/\pi af_o]^2$ as described in PR1. This variation is clearly evident in Figure 5 and contains information about the spot diameter a.

As pointed out in PR1, the power spectrum should also contain information about the separation distance d. This information is contained in a higher frequency modulation of the single hole transform. To see if this information is actually contained in Figure 5 a contact print of this power spectrum measurement was made and used as a signal in the optical processor. As shown in PR1 the transform of this power spectrum is proportional to the autocorrelation function of the original random pattern in Figure 4. Figure 6 shows the resulting autocorrelation function as measured in the transform plane of the optical processor. The circle surrounding the central peak has a radius proportional to d. This circle is a direct result of light being diffracted by the predicted modulations of the single hole pattern. A larger periodic pattern is also observed in the autocorrelation measurement. This results from the fact that the random two-hole patterns were actually arranged periodically on the scope when constructing Figure 4. This inherent periodicity while not obvious in Figure 4 due to the random orientation of each individual two-hole pattern becomes quite evident in the autocorrelation measurement.

This example shows that optical measurements of the power spectrum and autocorrelation function of a random spatial

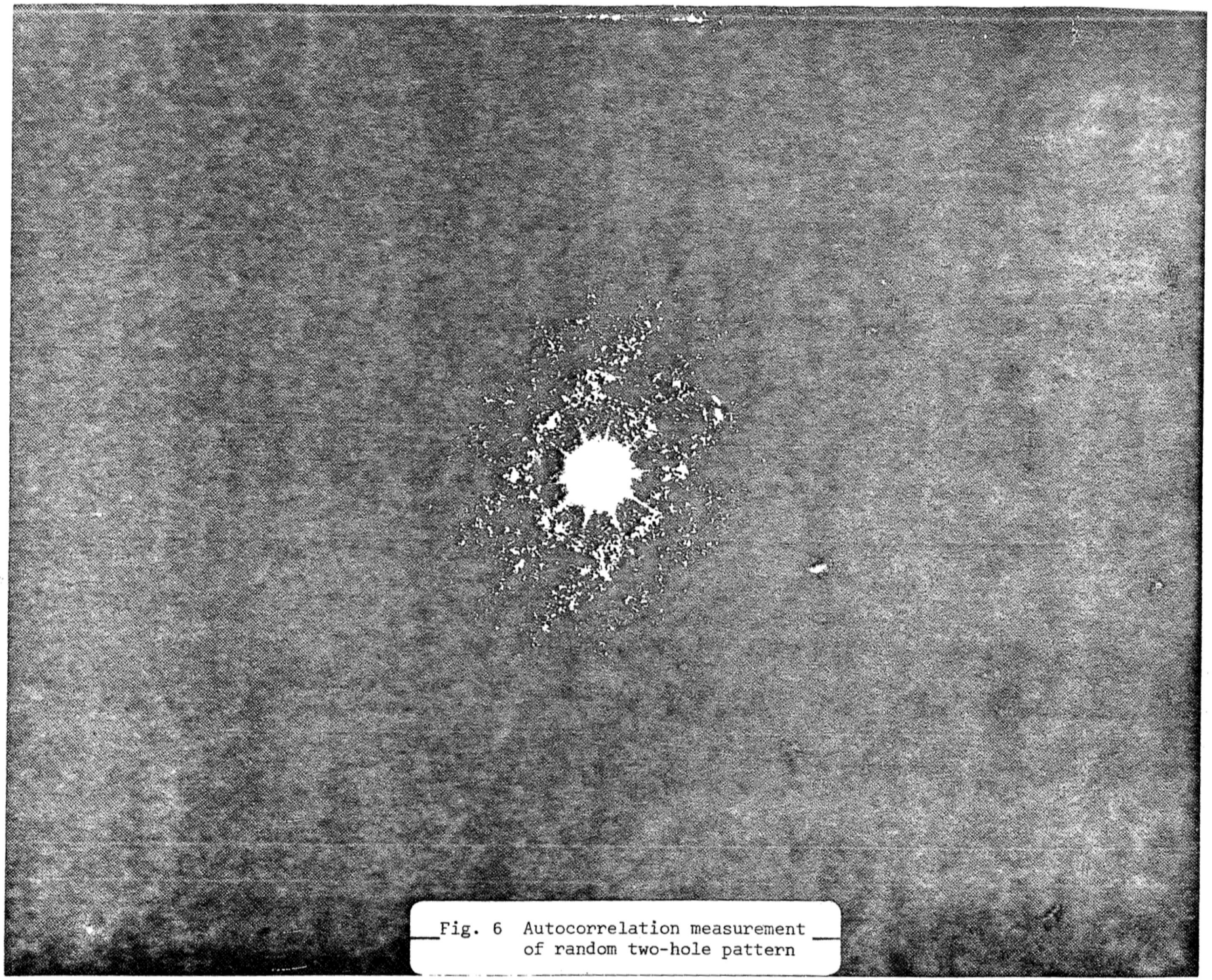

Fig. 6 Autocorrelation measurement of random two-hole pattern

pattern contain important information about the statistical nature of the random signal. This information can be used to recognize random patterns with certain prescribed statistical properties. The example also shows that often the autocorrelation (or in general a corss-correlation) measurement provides the most useful information for pattern recognition applications.

The two-step procedure used above for measuring the autocorrelation function is somewhat awkward and would be unsuitable in a real-time automatic control system application. What is needed for this case is a spatial filter in the transform plane proportional to $G^{*}(f)$ so that the autocorrelation function will appear instantaneously in the output plane. Such a filter can be made holographically which will then permit direct measurement of either the autocorrelation function or the cross-correlation with a known type of random pattern. Techniques are now being developed for making these types of spatial filters and using them for autocorrelation and cross-correlation meausrements.

References

1. Goodman, J. W., Introduction to Fourier Optics, McGraw-Hill: New York, 1968.

2. Born, M. and E. Wolf, Principles of Optics, 2nd Ed., Macmillan, New York, 1964.